JOURNAL OF MATERIALS SCIENCE 23 (1988) 2310–2320

Anisotropy of viscoelastic relaxations in a thermotropic rigid main chain polymer

H. J. ZIMMERMANN, J. H. WENDORFF
Deutsches Kunststoff-Institut, Darmstadt, West Germany

The dynamic mechanical properties of a thermotropic rigid chain polymer were investigated in the temperature range −150 to +150° C. The properties turned out to be highly anisotropic in oriented samples. Two relaxation processes, a strong secondary process and a weaker glass relaxation process, were found to influence the anisotropic dynamic mechanical properties in this temperature range both in the glassy nematic and in the crystalline state. The two relaxation processes couple, however, in a different manner to the mechanical properties in the nematic glassy, as compared to the crystalline state. It was also observed that the relaxation processes couple differently to the individual compliance constants within the same phase. The dynamic mechanical properties of the unoriented state could be predicted, to a first approximation, on the basis of an aggregate model, assuming a uniform stress distribution (Reuss average).

1. Introduction

Polymers which are composed of rigid chains and which exhibit a liquid crystalline phase at elevated temperatures have been found to display self-reinforcing effects, if processed from the anisotropic melt. These effects result from a spontaneous macroscopic orientation of the elongated chains during flow which does not readily relax even after the cessation of the flow. Parts can thus be manufactured by appropriate techniques which display a large stiffness and a large strength, at least along the axis of orientation. It might be speculated that such polymers are highly brittle, because of the strong restrictions imposed on conformational changes and thus on the mobility of segments.

The macroscopic mechanical, and also the dielectric and thermal properties of polymeric materials are known to be strongly controlled by the occurrence of molecular relaxation processes [1–6]. These processes give rise to stepwise variations of the tensile and shear elastic moduli within characteristic temperature ranges as well as to the dissipation of deformation energy. They control thus the brittle or ductile behaviour of the polymers.

Flexible chain polymers have been found to exhibit a large variety of different relaxation processes [1–6]. High-frequency rotational motions of end groups, rotational or translational rotational motions of side groups or of short segments within the backbone of the chain are just some examples. These high-frequency relaxation processes are usually thermally activated and display a temperature-independent activation energy [7]. They take place both in the glassy or in the crystalline state. In addition, lower frequency large-scale cooperative motions occur which incorporate motions of many segments including those of neighbouring chains. This process, the glass relaxation process, controls mechanical and nonmechanical properties to a great extent.

Now, for rigid chain molecules the expectation is that the total number of relaxation processes which can take place is strongly decreased in comparison to the case of flexible chain molecules. This should lead to an increased brittleness of such polymers at lower temperatures and to the absence of stepwise variations of the elastic moduli in the glassy or crystalline state at lower temperartures.

In addition, one expects a strong shift of the remaining relaxation processes, particularly of the glass relaxation, to higher temperatures as the chain stiffness increases. This argument is based on the assumption that the characteristic time scale of the relaxation process scales with the viscosity of the condensed – in our case anisotropic – amorphous phase [7, 8]. Most characteristic viscosity coefficients of the anisotropic condensed state are predicted to diverge with increasing chain length and chain stiffness [9, 10]. This should lead to a similar behaviour of the time scale of the relaxation process. Furthermore, one expects that the activation energies of molecular processes increase strongly with increasing chain stiffness due to the occurrence of correlated motions in the densely packed condensed phase of stiff chain molecules. Such an increase was observed, for instance for the α-process in liquid crystalline side chain polymers [11–13].

Surprisingly, most of the expectations described above are in disagreement with the experimental findings [14–16]. It was observed, for instance, that the glass relaxation processes of rigid chain molecules occur at temperatures close to those of flexible chain molecules of comparable chemical structure. It was furthermore found that rigid chain molecules are able to display rather strong low-temperature relaxations, very similar to those observed for flexible chain

0022–2461/88 $03.00 + .12

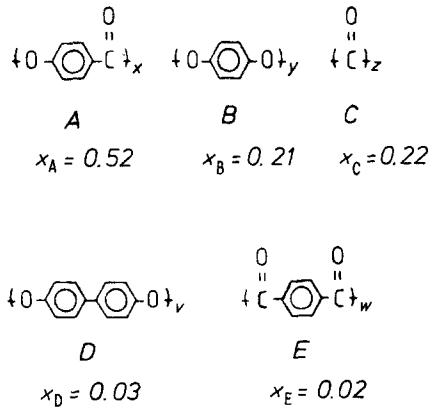

Figure 1 Chemical composition of the copolymer studied.

molecules. These cause a surprisingly large impact strength of such stiff chain polymers already at temperatures far below room temperature.

These unexpected findings motivated us to investigate the dynamic mechanical properties of rigid chain thermotropic polymers in detail over a large temperature range. We studied, in particular, the dependence of the individual complex compliance constants, characteristic of the oriented state, on the relaxation processes as well as the variations of the anisotropic viscoelastic properties with the degree of crystallinity. The polymer for which results are reported in this paper is a statistical copolymer, containing about 52 mol % hydroxybenzoic acid units, about 21 mol % hydroquinone and about 22 mol % diphenylcarbonate, and small concentrations of 4, 4′-dihydroxydiphenyl and terephthalic acid (Fig. 1). It displays a nematic phase at temperatures above about 300° C and a partially crystalline state at room temperature. The degree of crystallinity was found to vary between 25 and more than 70 wt %, depending on the annealing conditions. The particular structure of the crystalline state which enables the formation of a three-dimensional positional order, despite the irregular chemical structure of the polymer chain, has been discussed in detail in previous publications [16, 17]. A cocrystallization of the different structural elements shown in Fig. 1 takes place. The incorporation of these units causes the crystal to become rotationally disordered in the sense that the centres of gravity are located on a three-dimensional lattice whereas the molecules are rotationally disordered about the long axis of the chain. This state corresponds, in principle, to a plastic crystal state. In addition it was found that the crystal lattice parameters vary as a function of the annealing history. So the conclusion was that the relatively disordered crystalline state allows for the formation of a rather high degree of crystallinity within the copolymer system.

2. Experimental details

The experiments were performed on thin extruded films (thickness 135 μm) displaying a strong orientation of the chains along the extrusion direction. Rectangular samples were cut from these films in such a way that the chain orientation was either parallel or perpendicular to the long axis of the samples. This allowed the determination of the longitudinal and transverse complex shear moduli $G_\parallel^*$ and $G_\perp^*$ and longitudinal and transverse tensile moduli $E_\parallel^*$ and $E_\perp^*$. In addition, injection-moulded dog-bone shaped test bars were used for the experiments.

The complex shear modulus was determined within a temperature range -180 to $+150$° C at a frequency of some Hertz, employing a Zwick torsional pendulum. The tensile modulus was determined in a similar temperature range using a Vibron at frequencies between 1 and 100 Hz.

3. Experimental results

3.1. The texture of the samples

The X-ray diagram obtained for the injection-moulded bars showed that these display a weak orientation of the chain axis parallel to the injection direction. The orientation was found to be inhomogeneous throughout the cross-section of the sample. So the bars are rather ill-defined in terms of the structure. This is not the case, however, for the extruded films.

The X-ray results, which were reported in previous papers, revealed that the extruded film is characterized by a nearly complete orientation of the chain axis along the extrusion direction [17, 18]. The orientational order parameter, S, defined by

$$S = \langle (3\cos^2\theta - 1)/2 \rangle$$
$$= \tfrac{1}{2} \cdot \int [(3\cos^2\theta - 1) f(\theta)] \sin\theta \, d\theta$$

where $f(\theta)$ is the orientation distribution function and where θ is the angle between the molecular long axis and the preferred direction, was found to be 0.8 already in the molten state. Its value thus corresponded closely to that expected for the nematic phase of long rigid chain molecules. The X-ray diagrams obtained for the quenched and annealed samples corresponded to fibre diagrams for the case that the X-ray beam was normal to the extruded films. In addition, it was found that the X-ray diagrams obtained with the beam parallel to the extrusion direction were characterized by ring-shaped reflections. This shows that we may treat the film as a uniaxial structure with the axis along the extrusion or chain orientation direction.

The compliance tensor, S_{ij}^*, is given in this case by

$$\begin{pmatrix} S_{11}^* & S_{12}^* & S_{13}^* & 0 & 0 & 0 \\ S_{12}^* & S_{11}^* & S_{13}^* & 0 & 0 & 0 \\ S_{13}^* & S_{13}^* & S_{33}^* & 0 & 0 & 0 \\ 0 & 0 & 0 & S_{44}^* & 0 & 0 \\ 0 & 0 & 0 & 0 & S_{44}^* & 0 \\ 0 & 0 & 0 & 0 & 0 & S_{66}^* \end{pmatrix}$$

where S_{66}^* is given by $2(S_{11}^* - S_{12}^*)$.

The dynamic mechanical properties are thus determined by five independent complex compliances: S_{11}^*, S_{33}^*, S_{44}^*, S_{12}^*, S_{13}^*. We analysed four of them (see Appendix): S_{11}^*, S_{33}^*, S_{44}^*, S_{12}^*. These may be written as [19]

$$S_{ij}^* = S_{ij}' - iS_{ij}''$$
$$S_{ij}'' = S_{ij}' \tan\delta$$

They are related to the tensile moduli, $E_{\parallel}$ and $E_{\perp}$, as well as to the shear moduli, $G_{\parallel}$ and $G_{\perp}$, as follows [19]

$$S'_{33} = \frac{1}{E'_{\parallel}[(1 + \tan\delta)^2]}$$

$$S''_{33} = \frac{1}{E''_{\parallel}[(1 + \tan\delta)^{-2}]}$$

$$S'_{11} = \frac{1}{E'_{\perp}[(1 + \tan\delta)^2]}$$

$$S''_{11} = \frac{1}{E''_{\perp}[(1 + \tan\delta)^{-2}]}$$

$$S'_{44} = \frac{1}{G'_{\perp}[(1 + \tan)^2]}$$

$$S''_{44} = \frac{1}{G''_{\perp}[(1 + \tan)^{-2}]}$$

$$S'_{66} = \frac{1}{G'_{\parallel}[(1 + \tan)^2]}$$

$$S''_{66} = \frac{1}{G''_{\parallel}[(1 + \tan)^{-2}]}$$

Usually one assumes [19] that $-S^*_{13}/S^*_{33} = 0.5$ (ν_{13}), so one also gets values for these tensor components.

We investigated both the real (storage modulus) and the imaginary parts (loss modulus) of the moduli as well as the magnitude of the loss angle tan δ as a function of the temperature and the degree of crystallinity.

3.2. The complex shear modulus, G_i^* obtained for injection-moulded samples

The shear modulus obtained for the dog-bone shaped injection-moulded samples, displays two stepwise variations with increasing temperature, one in a temperature range around about $-35°$ C and the other in a temperature range around about 95° C. This is shown in Fig. 2. The stepwise variation of the storage modulus gives rise to the occurrence of a maximum for the loss modulus and for tan δ, as shown in Fig. 3. So apparently a low temperature and a high-temperature relaxation process occur in the thermotropic copolymer studied here. We will denote the high-temperature process by α and the low-temperature process by β, in the following.

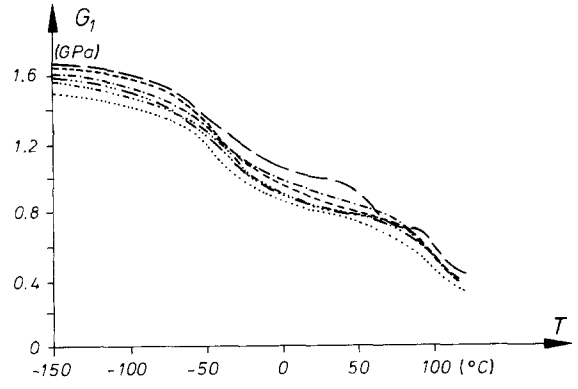

Figure 2 Torsional storage modulus G' for injection-moulded samples with varying degree of crystallinity: w_c = (——) 40%, (-·-·-·-) 44%, (- - - -) 49%, (— · · · —) 53%, (- · · · -) 55%, (· · ·) 58%, (— — —) 62%.

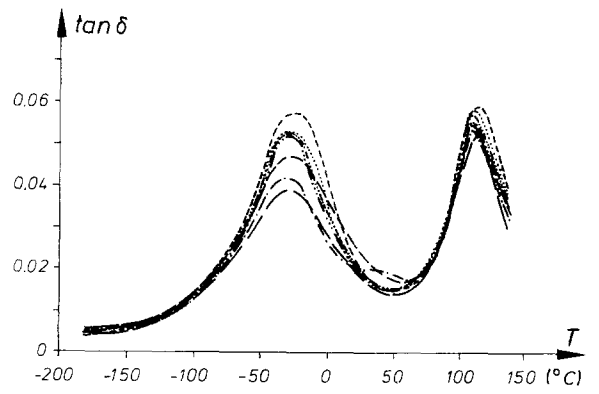

Figure 3 Torsional loss modulus G'' for injection moulded samples with varying degree of crystallinity: w_c = (——) 40% (-·-·—) 44%, (- - - -) 49%, (- · · · -) 53%, (— · · · —) 55%, (· · ·) 58%, (— — —) 62%.

Annealing of the polymer results in a strong increase of the degree of crystallinity [17, 18]. The observation is that this increase gives rise to a distinct increase in the height of the low-temperature (β) tan δ and G'' peak (Fig. 4) and only to a very weak variation of the height of the high temperature (α) tan δ and G'' peak (Figs 3, 4). The shear modulus G' is found, on the other hand, to be shifted to lower values with increasing degree of crystallinity over the whole temperature range (Fig. 2). The weak dependence of the properties of the high-temperature (α) relaxation on the degree of crystallinity is rather surprising. One usually expects a more or less linear increase or decrease of the strength of a relaxation with increasing degree of crystallinity. The reason is that the relaxation process is either characteristic of the amorphous or of the crystalline phase [1–6].

Detailed studies on the dependence of the dynamic mechanical properties of isotropic or weakly oriented samples cannot be expected to lead to a basic understanding of the properties of the relaxation processes

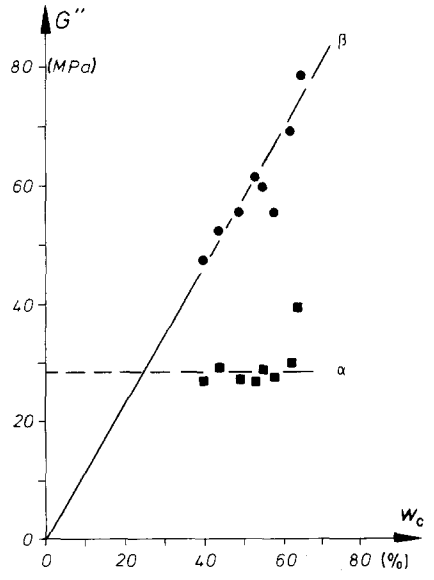

Figure 4 Absolute height of the α- and β-relaxation maximum as a function of the degree of crystallinity.

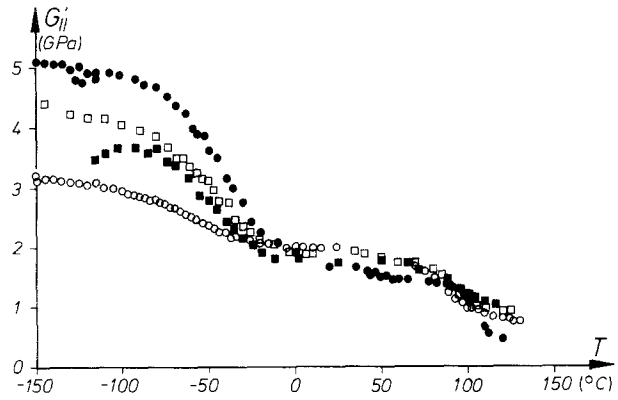

Figure 5 Torsional storage modulus of oriented samples with varying degrees of crystallinity (chains parallel to the torsional axis). w_c = (○) 35%, (■) 45%, (□) 60%, (●) 80%.

involved. This is particularly the case for thermotropic rigid chain molecules, because we know that they have to be locally highly anisotropic, due to their nematic state in the melt and in the glassy state. It is therefore necessary to perform experiments on oriented samples. These should enable us to obtain also information on the anisotropy of the molecular relaxation processes.

3.3. The complex shear modulus $G^*_{\parallel} = G'_{\parallel} + iG''_{\parallel}$

The shear modulus $G'_{\parallel}$ obtained for the highly oriented film is characterized, as in the case of the weakly oriented injection-moulded sample, by a stepwise variation in a temperature range around $-35°$ C and by a second stepwise decrease within a temperature range around 95° C. This is obvious from Fig. 5. The stepwise decrease of the shear modulus is accompanied in both cases by the occurrence of a maximum for the loss modulus G'' and for tan δ, as shown in Fig. 6.

A variation of the degree of crystallinity, as achieved by annealing the samples for prolonged times at elevated temperatures, gives rise to strong variations of the shear modulus, the loss modulus and tan δ. The low-temperature shear modulus is found to increase strongly with increasing degree of crystallinity, as is evident from Fig. 5. The variation of the modulus with increasing degree of crystallinity becomes, however, much weaker above a temperature

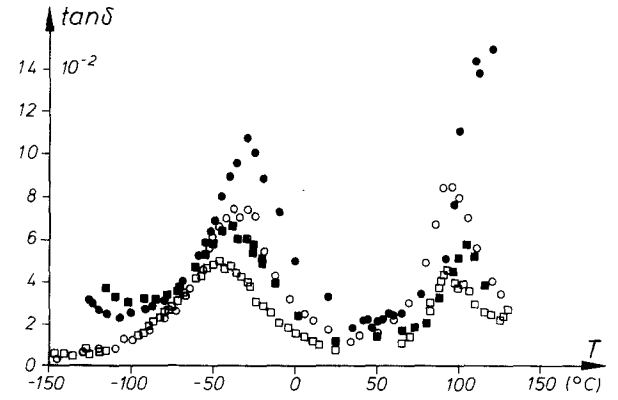

Figure 6 Torsional loss (tan δ) of oriented samples with varying degrees of crystallinity (chains parallel to the torsional axis). w_c = (○) 35%, (■) 45%, (□) 60%, (●) 80%.

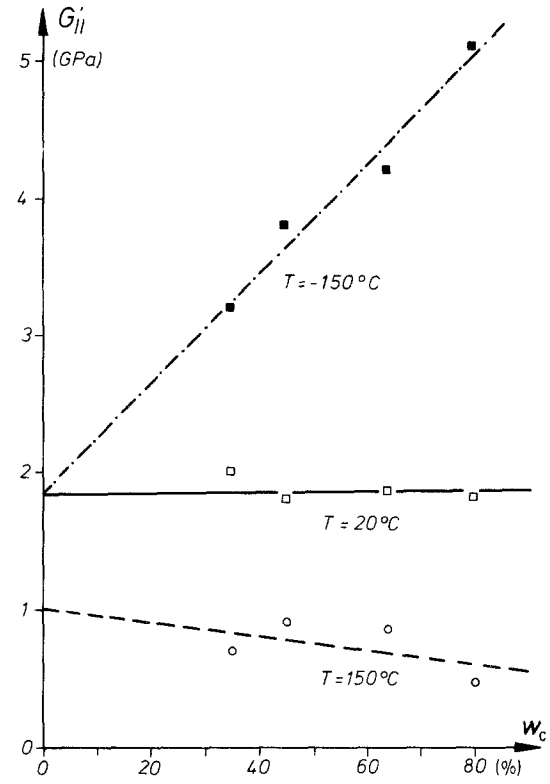

Figure 7 Torsional storage modulus for an oriented sample (chains parallel to the torsional axis) as a function of the degree of crystallinity for three selected temperatures.

of about $-20°$ C. This is obvious from Fig. 7 which shows the variation of the shear modulus with the degree of crystallinity at selected temperatures.

The increase of the degree of crystallinity results in a corresponding increase of the height of the tan δ peak related to the β-relaxation and in a less well-defined increase of the height of the tan δ peak related to the α-relaxation (Fig. 6).

The absolute magnitude of the stepwise decrease of the shear modulus due to the β-process is much larger than the corresponding magnitude of the decrease due to the α-process, at least for larger degrees of crystallinity (Fig. 5). The values for the relaxation strength, S_r, of the two relaxation processes, defined by

$$S_r = (G_u - G_r)/G_r$$

where G_r is the relaxed and G_u the unrelaxed modulus, are, however, of similar magnitude. They differ by a factor of less than two even in the case of highly crystalline samples.

3.4. The complex shear modulus $G^*_{\perp} = G'_{\perp} + iG''_{\perp}$

The shear modulus, $G'_{\perp}$, is also found to decrease stepwise within the same temperature ranges as the shear moduli G'_i and $G'_{\parallel}$. This is shown in Fig. 8. The corresponding variation of the loss modulus is shown in Fig. 9. Again a strong variation of the shear modulus $G'_{\perp}$ with increasing degree of crystallinity is observed. This is shown in Fig. 8 and 10. The observation is, however, that $G'_{\perp}$ increases with decreasing degree of crystallinity, in contrast to the case of the shear modulus $G'_{\parallel}$. This happens both in the low-temperature, and the high-temperature region. It

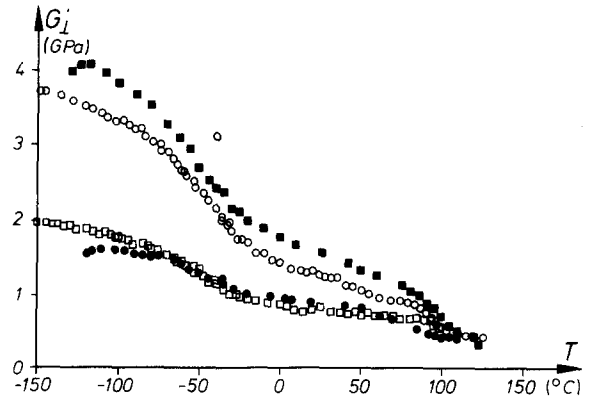

Figure 8 Torsional storage modulus of oriented samples with varying degree of crystallinity (chains vertical to the torsional axis). w_c = (○) 35%, (■) 45%, (□) 60%, (●) 65%.

corresponds to a decrease of the absolute value of the stepwise variation of the modulus, both for the α- and β-relaxation process and also to a decrease of the relaxation strength process and also to a decrease of the relaxation strength both of the α- and the β-process with increasing degree of crystallinity.

3.5. Additional characteristic properties of the α- and β-relaxation process

The location of the α-process on the temperature scale as well as the width on this scale were found to be approximately independent of the degree of crystallinity, both for the case of the highly oriented film and the weakly oriented test bar.

A definitely different result was obtained for the β-relaxation. Fig. 11a shows the width of the relaxation on the temperature scale as obtained for the particular case of the weakly oriented samples. A noticeable decrease of the width, indicative of a narrowing of the distribution of the relaxation times, is observed with increasing degree of crystallinity. In addition, one finds, in some instances, that the location of the β-relaxation is strongly shifted to high temperatures – which corresponds to a shift of the average relaxation time to lower frequencies – with increasing degree of crystallinity. This is shown in Fig. 11b for the case of a weakly oriented sample and for the case of the oriented film as far as the direction parallel to the orientation direction is concerned.

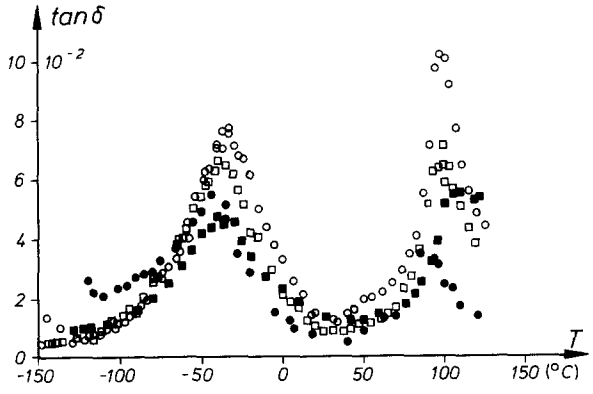

Figure 9 Torsional loss (tan δ) of oriented samples with varying degree of crystallinity (chains vertical to the torsional axis). w_c = (○) 35%, (■) 45%, (□) 60%, (●) 65%.

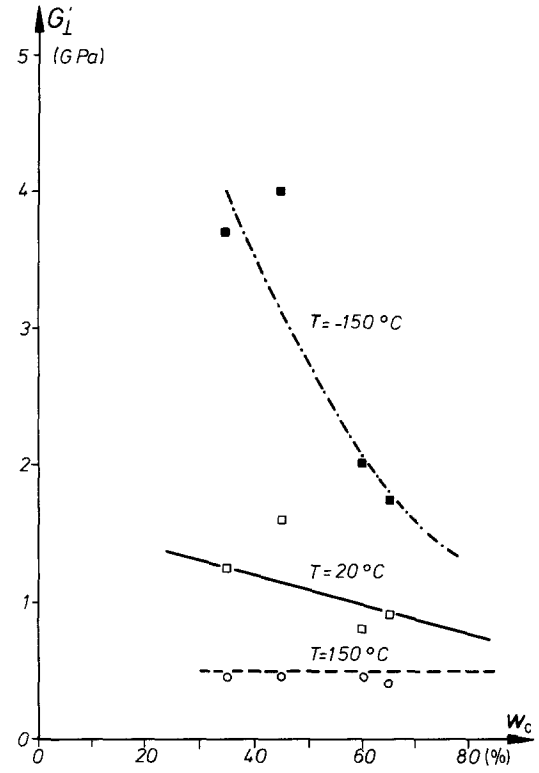

Figure 10 Torsional storage modulus for an oriented sample (chains vertical to the torsional axis) as a function of the degree of crystallinity for three selected temperatures.

No such variation was found, however, for the low-temperature relaxation controlling $G_\perp'$. On the contrary, a weak decrease of the relaxation temperature with increasing degree of crystallinity was observed in this case. This may be taken as an indication that the β-process is really a multicomponent process.

3.6. The complex tensile moduli E_i^*, $E_\parallel^*$ and $E_\perp^*$

The tensile moduli $E_\parallel^*$, $E_\perp^*$ were determined for the extruded films and the tensile modulus E_i^* for the injection-moulded bar (Figs 12 to 14). Each of these was characterized by a stepwise decrease of their magnitude with increasing temperature in a temperature range around about −35° C and about 95° C. The tensile moduli thus display similar properties as the shear moduli. The main difference between the three tensile moduli was their absolute magnitude. $E_\parallel'$, was found to be one order of magnitude larger in comparison to $E_\perp'$ and E_i', respectively. This is obvious from Figs 12 and 13. The last two moduli agree very closely with each other.

The magnitude of the relaxation strength as well as of the loss maximum were about equal for all three quantities, as can be seen in Fig. 14. The variation of the degree of crystallinity was found to give rise to only small variations of the dynamic tensile properties of the injection-moulded test bar, in agreement with the results obtained for the shear modulus.

3.7. Dielectric relaxation

The results of dielectric relaxation studies performed on the thermotropic copolymer discussed here have previously been published [18]. They also revealed the

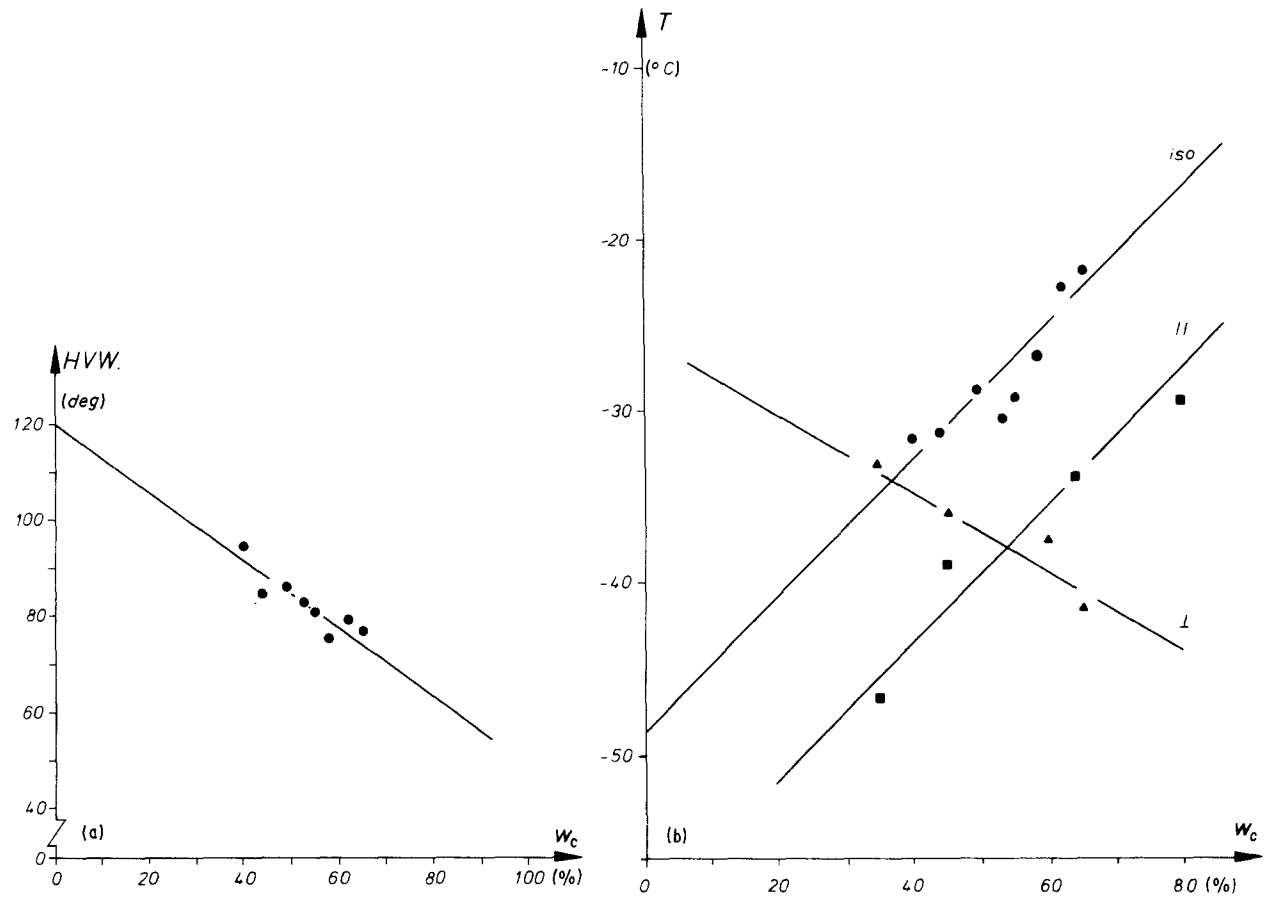

Figure 11 (a) Half value width of the β-relaxation maximum as a function of the degree of crystallinity for isotropic samples. (b) Temperature of the β-relaxation maximum as a function of the degree of crystallinity for (■) parallel oriented samples, (▲) vertically oriented samples, (●) injection-moulded samples.

presence of two relaxation peaks, corresponding to the low-temperature β-process and the high-temperature α-process, respectively. These results have to be taken as an indication that both relaxation processes posess not only translational but also rotational components of motion. The dielectric relaxation data were used to compose an activation diagram, which allows characterization of the two relaxation processes with respect to their nature, as discussed below.

4. Discussion

This section is concerned with the discussion of the influence of the α- and β-relaxation on dynamic mechanical properties. The absolute values of the stiffness constants will be discussed in the Appendix.

It is obvious that the dynamic mechanical properties of the rigid thermotropic polymer are strongly influenced by the presence of two distinct relaxation processes, one of which occurs below room temperature and one of which occurs above. We will discuss the influence of the β- and α-relaxation processes on the dynamical mechanical properties separately.

The low-temperature β-relaxation process causes the room-temperature shear and tensile moduli of the isotropic and weakly oriented samples to be smaller by a factor of about 2 in comparison to the corresponding

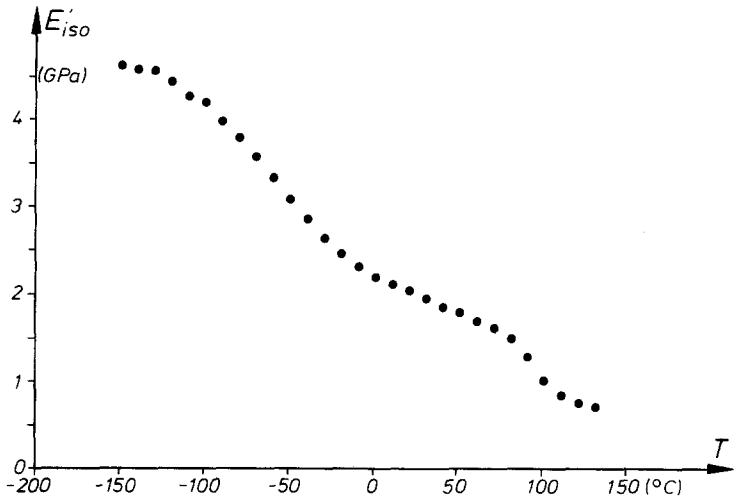

Figure 12 Tensile modulus of an isotropic sample.

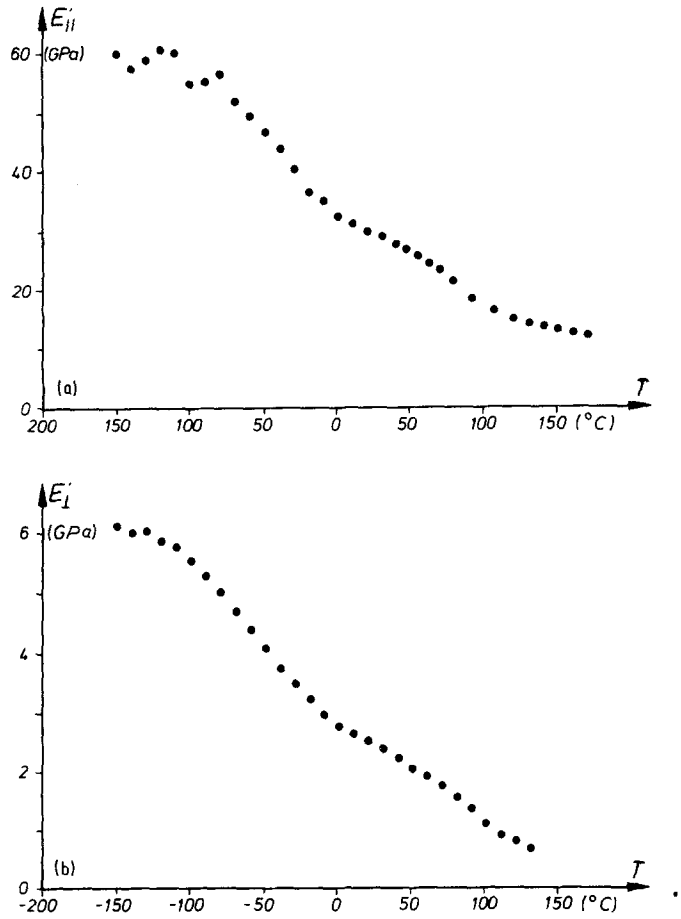

Figure 13 Tensile modulus of (a) an oriented sample, chains parallel to tensile direction, (b) an oriented sample, chains perpendicular to tensile direction.

values at low temperatures. This strong decay is rather surprising in view of the fact that we are considering rigid chain molecules.

Previous studies have revealed that the low-temperature β-process displays a temperature-independent activation energy, amounting to about 62.3 kJ mol^{-1}. This has to be taken as an indication that this process involves local motions and that these motions are intrachain motions. The chain molecules are thus not really rigid but possess some kind of dynamic freedom. The experimental results described above revealed that the relaxation process couples to shear properties, to tensile properties as well as to dielectrical properties. This shows clearly that the β-process possesses rotational as well as longitudinal and transverse translational components of motions.

A variety of flexible chain polymers such as polycarbonate, or of semiflexible chain thermotropic polymers as well as combined main chain side chain polymers, are known to display a low-temperature relaxation, characterized by an activation energy and a characteristic time scale which correspond closely to those found here for the rigid chain polymer [13, 19]. These processes were also found to couple strongly to mechanical and electrical properties. The β-relaxation process has been attributed for these polymers to mobile phenyl groups performing 180 deg flips and smaller angle fluctuations about the same axis [19]. Both the magnitude of the activation energy and of the characteristic time scale of these motions agree with those of the β-process in the rigid polymer. Therefore, it seems reasonable to assume that similar

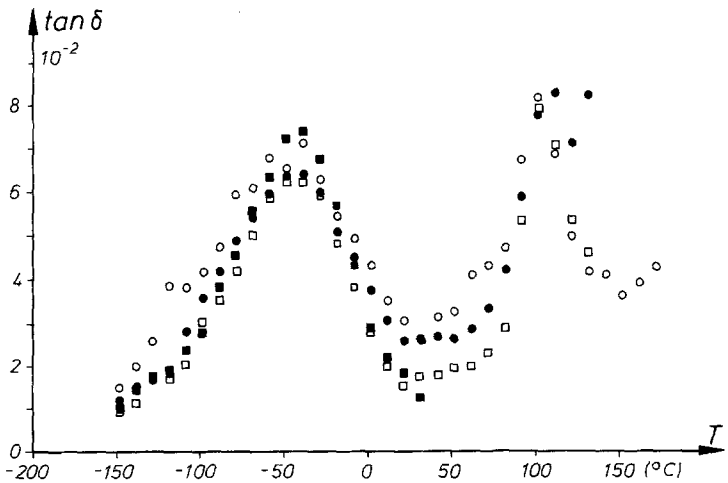

Figure 14 Tan δ (tensile) of (□) an isotropic quenched sample, (■) an isotropic annealed sample, and oriented samples, chains (○) parallel and (●) perpendicular to the tensile direction.

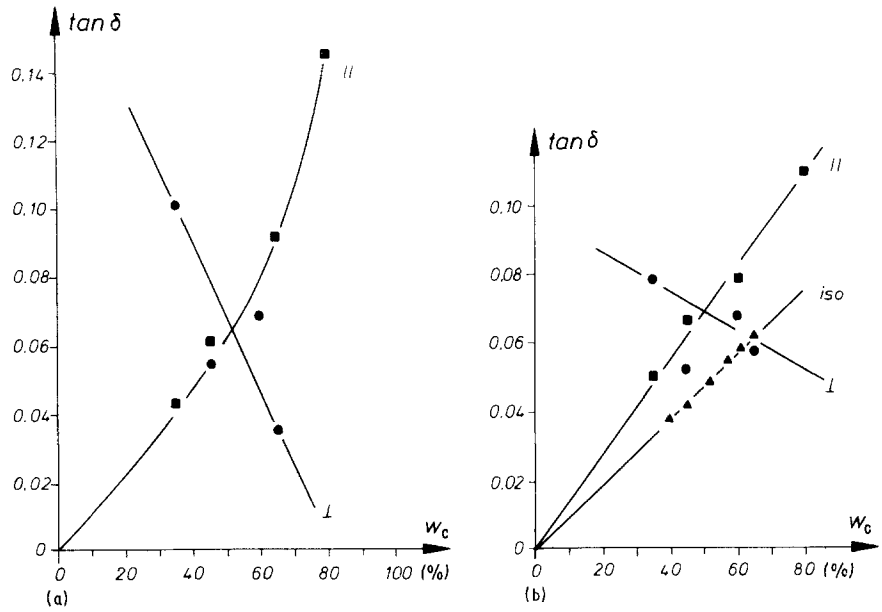

Figure 15 Tan δ (torsional) for (a) the α-relaxation and (b) the β-relaxation for oriented samples, chains (■) parallel and (●) perpendicular.

motions are responsible for the low-temperature decrease of the moduli of the rigid chain molecule considered here.

Such processes may well couple differently to different dynamic mechanical properties and may thus determine the frequency or temperature dependence of the different moduli in different ways. This is obviously the case for the polymer considered here. It was observed, for instance, that the height of the loss peak and the relaxation strength of the β-relaxation are much larger for $G'_{\parallel}$ than for $G'_{\perp}$, for highly crystalline samples (Figs 7, 10, 15) In addition, this anisotropy depends strongly on the degree of crystallinity. This is also obvious from Figs 7, 10 and 15. It was found, for instance, that the relaxation strength of the β-process increased with increasing degree of crystallinity for the case of the shear modulus, $G'_{\parallel}$, and that the relaxation strength increased with decreasing degree of crystallinity for the shear modulus, $G'_{\perp}$. These results show, first of all, that the relaxation process is present both in the nematic glassy state and in the crystalline state and secondly that it apparently couples differently to the macroscopic dynamic mechanical properties in the two states.

Before discussing this in more detail, the influence of the high-temperature α-process on the mechanical properties will be considered. The characteristic properties of the α-process correspond to those of a typical glass relaxation process. It involves thus large scale cooperative translational and rotational motions. The α-process causes an additional decay of the shear and the tensile moduli at higher temperatures in addition to that originating from the β-process. The process is highly anisotropic and depends strongly on the degree of crystallinity. This is evident from Figs 7, 10 and 15.

So it is apparent that the two relaxation processes influence the dynamic mechanical properties of the rigid chain molecules in a very complex way. In order to be able to draw direct information on the influence of the relaxation processes on dynamic mechanical data both as a function of the orientation and the degree of crystallinity, we used the plots shown in Figs 4, 7, 10 and 15 to obtain the corresponding dynamic mechanical properties of the pure nematic glassy state and of the pure crystalline state, based on an extrapolation. The linear variation of the magnitude of the storage and loss moduli with the degree of crystallinity, w_c, found for a limited range of w_c values, suggests that such an extrapolation will not meet with too strong uncertainties. The idealized curves obtained in this way are shown in Fig. 16a and b for the storage moduli $G'_{\parallel}$ and $G'_{\perp}$ along the perpendicular to the chain axis orientation and in Fig. 17 for the injection-moulded bar. We will first discuss the results obtained for the oriented structures.

The predictions are that the low-temperature shear modulus, $G'_{\parallel}$, is large for a crystalline material and much lower for the nematic glassy state. This difference vanishes, however above the temperature range in which the β relaxation occurs. So it is evident that the β-relaxation couples strongly to the shear modulus, $G'_{\parallel}$ (Fig. 16) only in the crystalline state. The α-process, on the other hand, apparently couples with about equal magnitude to $G'_{\parallel}$ both in the crystalline and in the nematic glassy state.

Just the opposite behaviour is observed for the shear modulus, $G'_{\perp}$. It is found to be large at low temperatures for the glassy nematic phase and quite small for the crystalline state. So, one finds that the β-relaxation process and also the α-process couple to the shear modulus, $G'_{\perp}$, only in the nematic glassy state. The shear modulus, $G'_{\perp}$, of the crystalline state does not couple at all to relaxation processes in the whole temperature range studied. The shear moduli, $G'_{\perp}$, of the two phases, i.e. of the nematic and the crystalline phase, become approximately equal above the temperature at which the α-process takes place.

Finally we consider the case of the injection-moulded sample, displaying only a weak and heterogeneous orientational order. The extrapolation leads to the result that the shear moduli both of the crystalline and the nematic state are of similar magnitude at low temperatures and above room temperature and depend in a similar way on the temperature, as depicted in

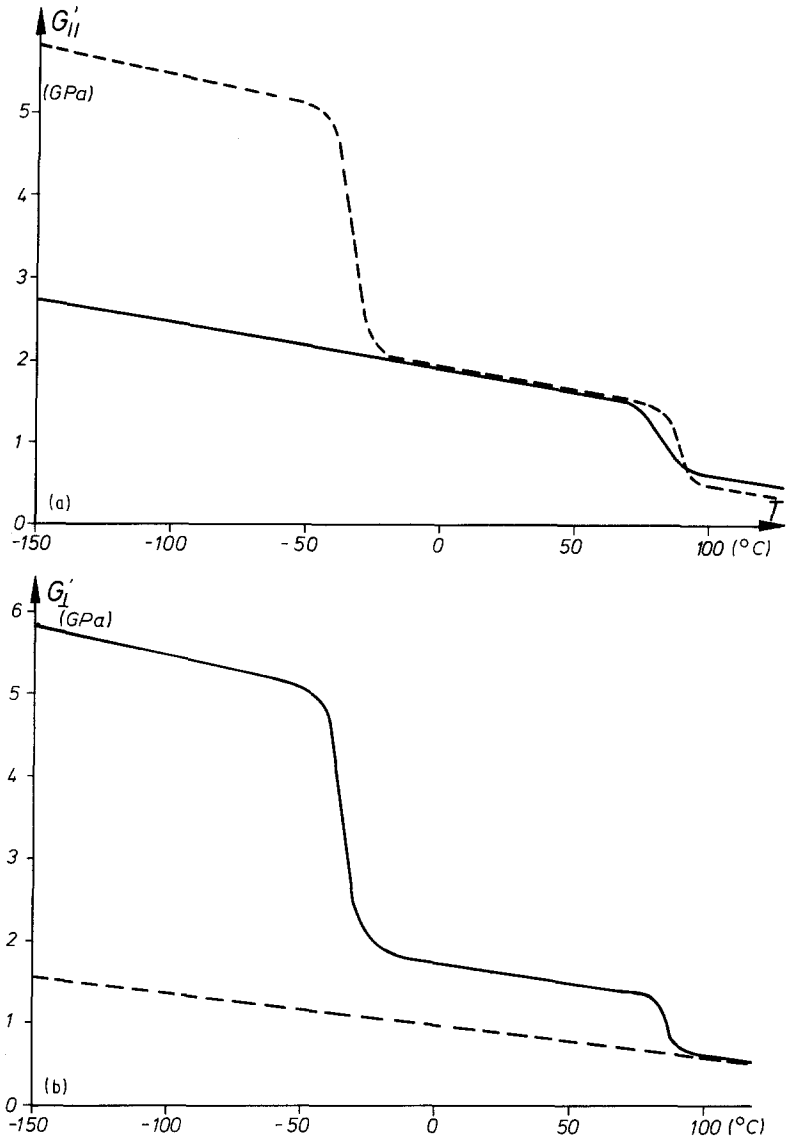

Figure 16 Extrapolated torsional storage modulus of the oriented sample (a) chains parallel to the torsional axis and (b) chains perpendicular to the torsional axis, for (– – –) the purely crystalline state and (——) the purely glassy nematic state.

Fig. 17. The only difference which is evident is that the crystalline phase shows a distinct low-temperature stepwise variation of the magnitude of the shear modulus $G_{\perp}'$ whereas it is smeared out on the temperature scale for the case of the glassy nematic phase. This has to be taken as an indication that the glassy nematic state is characterized by a broader distribution of the relaxation times of the β-process.

It is apparent that both the β-process and the α-process occur in the nematic glassy state as well as in the crystalline state. This is the reason why the dynamic mechanical properties such as the shear and tensile and also the dielectric properties of the only weakly oriented injection-moulded sample do not change strongly with the degree of crystallinity.

We found, on the other hand, however, that the highly oriented samples display strongly anisotropic dynamic properties which depend on the degree of crystallinity. The conclusion has to be that the nature of the environment of the relaxing species does not control the relaxation process but rather its coupling to macroscopic dynamic mechanical properties. The nature of the coupling seems, furthermore, to be different for the case of the α- and for the case of the β-relaxation.

In the following paragraphs we will present a tentative model which might be able to account for the anisotropic properties of the relaxation process and for the dependence of the coupling on the environment.

The freezing-in of the motions characteristic of the β-process leads obviously to a strong restriction of local sliding processes along the chain axis for the crystalline state and to a strong restriction of local sliding motions in the transverse direction in the case of the nematic glass. There is no corresponding effect of the freezing-in of these motions on the local longitudinal sliding motion in the nematic phase and on the transverse sliding in the crystalline phase.

We know that the crystalline state is characterized by a perfect chain orientation and a longitudinal registry of neighbouring chains [17, 18]. The lateral order, on the other hand, is characterized by a rotational disorder of the chains about their long axis. The local flipping motions of the phenyl groups obviously allow the chains in the crystals to slide past each other despite the registry. The freezing-in of these motions consequently restricts these kinds of motions. The freezing-in of these flipping motions obviously does not restrict longitudinal sliding motions in the nematic phase, due to the only weak registry of neighbouring chains in this phase.

The transverse sliding motion obviously is possible

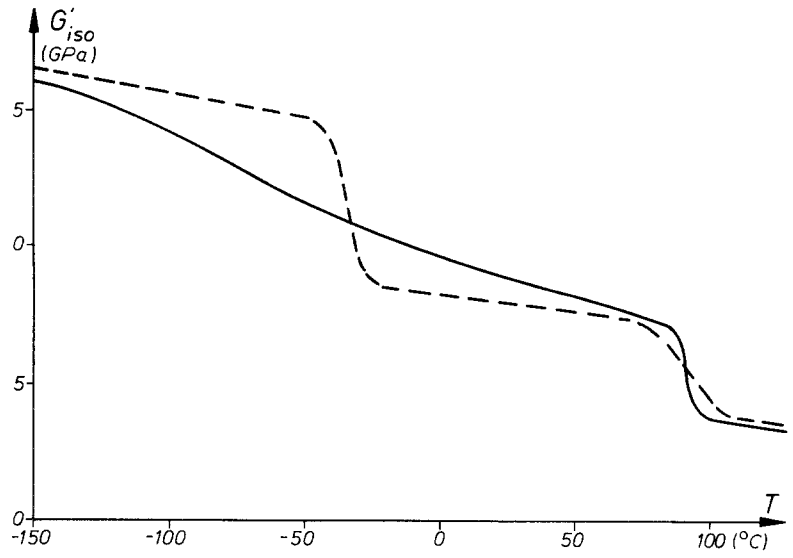

Figure 17 Extrapolated torsional storage modulus of the isotropic sample for (– – –) the pure crystalline state and (——) the pure glassy nematic state.

in the crystalline state even in the absence of such slipping motions because of the presence of rotational disorder and because of the parallelism of the chains. The orientational disorder of the chain axes, characteristic of the nematic phase, obviously restricts the possibility of transverse sliding motions, requiring thus the flipping motions in order for such motions to occur.

In a similar way we may account for the anisotropy of the dynamic mechanical properties, arising from large-scale cooperative motions (α-relaxational) of several chain units, probably belonging to different chains. This process couples equally to the longitudinal shear modulus, $G'_{\parallel}$ in the crystalline and in the nematic state but differently for the transverse shear modulus. So the sliding motion along the chain axis requires the presence of the cooperative motions both in the crystalline and in the nematic phase. The transverse sliding motions requires this process in the nematic phase but not in the crystalline phase. We may explain this difference in the same way as was done above for the case of the β-relaxation.

Finally, we will consider the variations of the relaxation properties of the β-relaxation as a function of the environment. The observation is that the process shifts to higher temperatures, i.e. becomes slower as the degree of crystallinity increases (Fig. 11). This is observed, however, only if we consider the modulus for the oriented material and if we consider $G'_{\parallel}$ for the isotropic or weakly oriented material. It stays about constant, if we analyse the transverse shear modulus $G'_{\perp}$. This seems to indicate that the β-process is not a simple process but may be composed of different motions, which couple differently to the different shear moduli.

TABLE I Experimentally obtained values for E', E'', G' and G'' at 25 and 200° C

	−200° C	25° C
E' (GPa)	60	29
E'' (GPa)	6.0	2.4
G' (GPa)	3.4	1.8
G'' (GPa)	4.0	1.1

Appendix. Determination of the compliances, S_{ij}, or stiffness constants, C_{ij}

Based on the equations given in Section 3, we calculated the compliances, S_{ij}, and stiffness constants, C_{ij}, for the highly oriented quenched samples at three reference temperatures, namely −150° C (i.e. below the temperature at which the β-relaxation takes place), 20° C (i.e. at a temperature between the glass transition and the low-temperature transition) and 150° C (i.e. well above the glass transition temperature). These values are shown in Table I. They are of the same order of magnitude as found for highly oriented polymers such as PETP, POM or PA 6. This is obvious from the data shown in Table II. The main difference between these flexible chain polymers and the rigid chain polymers is the ease with which a high orientational order can be induced in rigid chain molecules.

The stiffness constants and compliances displayed in Table I were used to calculate the tensile modulus and the shear modulus for isotropic samples on the basis of the aggregate model [18, 20]. In the aggregate model one either assumes a uniform stress distribution within anisotropic aggregates, which are randomly oriented in the isotropic phase (Reuss average) or one assumes a uniform strain (Voigt average). This corresponds either to an averaging of the compliance constants

$$\overline{S^i_{33}} = \tfrac{8}{15} S_{11} + \tfrac{1}{5} S_{33} + \tfrac{2}{15}(2S_{13} + S_{44})$$

$$\overline{S^i_{44}} = \tfrac{14}{15} S_{11} - \tfrac{2}{3} S_{12} - \tfrac{8}{15} S_{13} + \tfrac{4}{15} S_{33} + \tfrac{2}{5} S_{44}$$

(Reuss model)

TABLE II Compliances (10^{-10} m^2 N^{-1}) as obtained from the data given in Table I

	−200° C	25° C	PETP (highly oriented)
S_{11}	1.70	4.17	16
S_{33}	0.17	0.34	0.71
S_{44}	3.03	5.56	13.6
S_{12}	−0.50	1.1	−5.8
S_{13}	−0.09	−0.17	−0.31

TABLE III Predictions on the tensile and shear modulus of the isotropic samples for $T = -200°C$ and $T = 25°C$

	Uniform stress (Reuss)		Uniform strain (Voigt)	
	$-200°C$	$25°C$	$-200°C$	$25°C$
E' (GPa) predicted	7.58	3.35	11.70	5.72
observed	5.50	2.00	5.50	2.00
G' (GPa) predicted	3.10	1.40	8.46	4.04
observed	1.60	1.00	1.60	1.00

or to an averaging of the stiffness constants

$$\overline{C_{33}^{i}} = \tfrac{8}{15} C_{11} + \tfrac{1}{5} C_{33} + \tfrac{4}{15} (2 C_{13} + C_{44})$$

$$\overline{C_{44}^{i}} = \tfrac{7}{30} C_{11} - \tfrac{1}{6} C_{12} - \tfrac{2}{15} C_{13} + \tfrac{1}{15} C_{33} + \tfrac{2}{5} C_{44}$$

(Voigt model)

The results obtained on the basis of the two models are displayed in Table III. It is obvious that the Reuss model leads to a much better agreement between the predicted and the experimentally obtained values. This is obvious from Table III. So it seems that the structure of the isotropic state can be modelled by a series model rather than by a parallel model. One observes, however, that the observed values are still lower than those predicted by either of the models. This indicates that the extrusion giving rise to the macroscopical anisotropic state also induces some changes within the aggregates themselves.

Acknowledgement

We gratefully acknowledge the financial support of this work by the Bundesforschungsministerium für Forschung und Technologie (BMFT).

References

1. N. G. McCRUM, B. E. READ and G. WILLIAMS, "Anelastic and Dielectric Effects in Polymeric Solids" (Wiley, London, 1963).
2. R. T. BAILEY, A. M. NORTH and R. A. PETHRICK, "Molecular Motions in High Polymers" (Clarendon, Oxford, 1981).
3. P. HEDVIG, "Dielectric Spectroscopy of Polymers" (Hilger, Bristol, 1977).
4. G. M. BARTENEV and Y. V. ZELENEV, "Relaxation Phenomena in Polymers" (Wiley, New York, 1974).
5. I. M. WARD, "Mechanical Properties of Solid Polymers" (Wiley, New York, 1971).
6. *Idem.*, "Structure and Properties of Oriented Polymers" (Applied Science, London, 1975).
7. J. D. FERRY, "Viscoelastic Properties of Solid Polymers" (Wiley, New York, 1970).
8. F. BUECHE, "Physical Properties of Polymers" Interscience, New York, 1962).
9. P. G. de GENNES, "The Physics of Liquid Crystals" (Clarendon, London, 1979).
10. R. B. MEYER, in "Polymer Liquid Crystals", edited by A. Cifferi, W. R. Krigbaum and R. B. Meyer (Academic, New York, 1982).
11. W. HAASE, H. PRANOTO and F. J. BORMUTH, *Ber. Bunsenges. Phys. Chem.* **89** (1985) 1229.
12. R. ZENTEL, G. R. STROBL and H. RINGSDORF, *Macromolecules* **18** (1985) 960.
13. L. MONNERIE, *Pure. Appl. Chem.* **57** (1985) 1563.
14. B. WUNDERLICH and J. GREBOWICZ, *Adv. Polym. Sci.* **60** (1983) 1.
15. M. Y. CAO and B. WUNDERLICH, *J. Polym. Sci., Polym. Phys. Edn* **23** (1985) 521.
16. T. H. SAUER, H. J. ZIMMERMANN and J. H. WENDORFF, *ibid.* **25** (1987) 2471.
17. H. BECHTOLDT, H. J. ZIMMERMANN and J. H. WENDORFF, *Makromol. Chem.* **188** (1987) 651.
18. Z. H. STACHURSKI and I. M. WARD, *J. Polym. Sci.* **A2** (1968) 1083.
19. E. W. FISCHER, G. P. HELLMANN, H. W. SPIESS, F. J. HÖRTH, U. ECARIUS and M. WEHRLE, *Macromol. Chem. Suppl.* **12** (1985) 189.
20. Z. H. STACHURSKI and I. M. WARD, *J. Macromol. Sci. Phys.* **B3** (1969) 427.

Received 22 December 1986
and accepted 16 December 1987